HHS Public Access

Author manuscript

Stem Cell Res. Author manuscript; available in PMC 2016 November 01.

Published in final edited form as:

Stem Cell Res. 2015 November ; 15(3): 598–607. doi:10.1016/j.scr.2015.10.005.

MMP14 as a novel downstream target of VEGFR2 in migratory glioma-tropic neural stem cells

Nikita G Alexiades[1,⊥], **Brenda Auffinger**[1,⊥], **Chung Kwon Kim**[1], **Tanwir Hasan**[1], **Gina Lee**[1], **Marc Deheeger**[1], **Alex L. Tobias**, **Janice Kim**[1], **Irina Balyasnikova**[1], **Maciej S Lesniak**[1], **Karen Aboody**[2], and **Atique U Ahmed**[1,*]

[1]The Department of Surgery and the Brain Tumor Center, The University of Chicago, Chicago, Illinois, USA

[2]Department of Neuroscience, City of Hope National Medical Center and Beckman Research Institute, Duarte, California, USA

Abstract

Neural stem cell (NSC)-based carriers have been presented as promising therapeutic tools for the treatment of infiltrative brain tumors due to their intrinsic tumor homing properties. They have demonstrated the ability to migrate towards distant tumor microsatellites and effectively deliver the therapeutic payload, thus significantly improving survival in experimental animal models for brain tumors. Despite such optimistic results, the efficacy of NSC-based anti-cancer therapy has been limited due to the restricted tumor homing ability of NSCs. To examine this issue, we investigated the mechanisms of tumor-tropic migration of an FDA-approved NSC line, HB1.F3.CD, by performing a gene expression analysis. We identified vascular endothelial growth factor-A (VEGFA) and membrane-bound matrix metalloproteinase (MMP14) as molecules whose expressions are significantly elevated in migratory NSCs. We observed increased expression of VEGF receptor 2 (VEGFR2) in the focal adhesion complexes of migratory NSCs, with downstream activation of VEGFR2-dependent kinases such as p-PLCγ, p-FAK, and p-Akt, a signaling cascade reported to be required for cellular migration. In an in vivo orthotopic glioma xenograft model, analysis of the migratory trail showed that NSCs maintained expression of VEGFR2 and preferentially migrated within the perivascular space. Knockdown of VEGFR2 via shRNAs led to significant downregulation of MMP14 expression, which resulted in inhibited tumor-tropic migration. Overall, our results suggest, for the first time, the involvement of VEGFR2-regulated MMP14 in the tumor-tropic migratory behavior of NSCs. Our data warrant investigation of MMP14 as a target for enhancing the migratory properties of NSC carriers and optimizing the delivery of therapeutic payloads to disseminated tumor burdens.

[*]To Whom Reprint Request Should Be Addressed: The Brain Tumor Center, The University of Chicago Pritzker School of Medicine, 5841 South Maryland Ave, M/C 3026, Chicago, IL 60637; Tel (773) 702-0680; Fax (773) 834-2608, aahmed@surgery.bsd.uchicago.edu.

[⊥]These authors contributed equally.

Disclosure of Potential conflicts of Interest

The authors declare no competing financial interests

Introduction

Despite recent advances in the field of oncology, the most common primary malignant brain tumor in adults, glioblastoma multiforme (GBM), still carries a dismal prognosis 1. Its median survival remains just 12–15 months [1,2]. This is mainly due to the infiltrative nature of GBM, which hampers complete surgical resection, and the limited number of available anticancer agents that can effectively cross the blood brain barrier (BBB) and reach infiltrative tumor foci[2]. In this context, a novel platform of neural stem cell (NSC)-based targeted therapy towards disseminated tumors in the brain has emerged as a promising therapeutic modality. NSCs are self-renewing, multipotent cells that have the potential to differentiate into the three fundamental types of central nervous system (CNS) cells: neurons, astrocytes, and oligodendrocytes [3–8]. Three main intrinsic properties of NSCs that make them invaluable carriers of therapeutic payloads have so far been described. First is their inherent tumor homing capacity, which allows for migration of long distances throughout the brain to effectively achieve diffuse tumor burdens [9,10]. Second is their ability to function as targeted cell carriers [4,11–13], which allows them to be genetically engineered to express increased levels of therapeutic proteins [14,15]. In addition, they can be loaded with selective tumor-targeting agents (i.e. drugs, nanoparticles, oncolytic virus), while maintaining their tumor homing ability [14,15]. Third is their intrinsic immunosuppressive properties, which allow them to effectively deliver therapeutic payloads to infiltrative tumor areas while providing protection from the host immunosurveillance [11,16,17]. After extensive preclinical evaluation, the Food and Drug Administration (FDA) has approved the use of HB1.F3.CD NSCs in a phase I clinical trial for the treatment of recurrent high-grade gliomas (NCT01172964). HB1.F3.CD is a human-derived NSC line that was genetically engineered to express the suicide gene cytosine deaminase (CD), which converts the pro-drug 5-fluorocytosine (5-FC) into the chemotherapy agent fluorouracil (5-FU) [9,18]. Our laboratory has also extensively evaluated NSCs as targeted carriers for anti-glioma oncolytic virotherapy. A number of FDA-guided preclinical studies were conducted and this new therapeutic approach has now been approved for a Phase I clinical trial [4,11,17].

The main drawback of NSC-based anti-tumor therapies is that, despite the effective tumor tropism exhibited by NSCs, only small portions of transplanted cells can migrate towards the tumor. Several recent publications have revealed that 70–80% tumor volume reduction can be achieved in various orthotopic GBM xenograft models [18,19] even when only 20–30% of implanted HB1.F3.CD NSCs are able to effectively migrate from their implantation site to the tumor area [4,19–22]. Enhancing such homing capacity will likely be one of the critical goals for the fulfillment of the preclinical promise of NSC-based anti-cancer therapeutic strategies. The mechanisms that guide selective tumor-tropic NSC migration are yet to be completely understood. Recent data from our lab and others have suggested that chemokines and pro-angiogenic factors produced by the tumor microenvironment may serve as chemoattractants [4,23]. It has been shown that NSCs preferentially distribute within hypoxic areas in intracranial glioma xenografts. In addition, hypoxia inducible factor 1 alpha (HIF-1α) knockdown in glioma cells prevented the hypoxia-induced recruitment of NSCs [20]. This impaired migration was due to decreased vascular endothelial growth factor (VEGF), stromal cell-derived factor-1 (SDF-1), and urokinase-type plasminogen activator

(uPA) expression in tumor cells [20]. It was also demonstrated that intratumoral upregulation of VEGF induced a long-range attraction of transplanted human NSCs from distant sites in the adult brain [24]. In addition to VEGF, activation of MMPs has also been pointed as a mechanism of hypoxia-mediated NSC tropism to malignant areas [20,25,26]. Taken together, these data indicated that tumor-derived hypoxia-inducible chemo-attractant factors play a critical role in promoting tumor-tropic migration of NSCs. However, the downstream signaling pathways involved in this targeted migration remain to be elucidated. Therefore, the goal of this paper is to understand why only certain implanted NSCs possess migratory capacity. We also aim to establish a mechanism that can be leveraged as a possible target to enhance NSC migration and payload delivery capacity to the diffuse tumor burdens through selective overexpression of such molecule. Here we examined both the migratory and non-migratory fraction of NSC populations with functional assays, both in vitro and in vivo. Based on an array based analysis data presented here suggest MMP14 as a novel functional downstream target of VEGFA and VEGFR2 signaling, driving NSC migration and homing to targeted tumor areas.

Materials and Methods

Cell culture and propagation

The HB1.F3.CD, a *v-myc* immortalized human neural stem cell line, has been utilized in all experiments [27]. The human glioma cell lines U251, U87, and A172 were purchased from the American Type Culture Collection (Manassas, VA, USA). Cells were maintained in culture in Dulbecco's Modified Eagle's Medium (DMEM) with 2 mmol/l L-glutamine (Mediatech, Manassas, VA, USA) supplemented with 10% fetal bovine serum (FBS; Atlanta Biologicals, Lawrenceville, GA, USA) and 2% penicillin-streptomycin antibiotic (Cellgro, Manassas, VA, USA). The patient-derived GBM43 xenografted glioma specimens were provided by Dr. David James from the University of California San Francisco and maintained according to the published protocol [28]. All cell lines mentioned were enzymatically dissociated using 0.25% trypsin/2.21 mmol/l EDTA solution (Mediatech) and were grown at 37ºC and 5% CO_2 humidified atmospheric conditions.

Evaluation of NSC migration

To evaluate the migratory characteristics of NSCs *in vitro*, we used a similar system described previously [29], with slight modifications. BD Biocoat Tumor Invasion System containing BD Falcon Fluoroblock 24-Multiwell inserts (8-μm pore size; PET membrane) was used following the manufacturer's instructions (BD Biosciences, Bedford, MA, USA). The migration of GFP-labeled NSCs was characterized towards conditioned media obtained by culturing 5×10^4 GBM43 cells in serum-free/growth factor-free media for 24 hours. The medium was added to the bottom well of the migration chamber to act as a chemoattractant. NSCs were then plated in the top insert at a density of 3×10^5 cells per well in DMEM (Mediatech, Manassan, VA) along with 5×10^4 glioma cells in the lower chamber of the 24-well plate; the cells were kept in these conditions for 48 hours. Cells located above the migration filter were classified as non-migratory and those just below the filter as migratory; each group of cells was collected by using cell scrapers for subsequent gene expression, qRT-PCR, and flow cytometry analysis. The number of migrating cells in three random

fields of views per well was counted using an Olympus IX81 inverted microscope (original objective: 20X) and analyzed using the MetaMorph software (Olympus, Tokyo, Japan).

Western blot analysis

HB1.F3.CD cells were incubated with various concentrations of VEGF recombinant protein for 30 minutes or with 100 ng/ml of VEGF for increasing time periods. Cells were washed and harvested in 1X Phosphate Buffered Saline (PBS; Cellgro) and subsequently lysed with lysis buffer (M-PER Mammalian Protein Extraction Reagent; Pierce, Rockford, IL, USA) supplemented with 10 mmol/L Protease and Phosphatase Inhibitor cocktail (Roche, Indianapolis, IN, USA) according to the manufacturers' instructions. Thirty μg of cell lysate per well were subjected to SDS-PAGE electrophoresis and transferred to PVDF-membrane for immunoblotting (Bio-Rad, Hercules, CA, USA). Subsequently, transferred proteins were labeled with anti-p-VEGFR2, p-PLCy1, p-FAK, p-Src, p-Akt, Akt, p-ERK1/2, and p-p38 antibodies from the Angiogenesis Antibody Sampler Kit (Cell Signaling Technology, Beverly, MA, USA) as well as anti-human MMP-14 (Abcam, Cambridge, MA, USA). The bound antibodies were visualized with enhanced chemiluminescence reagent (Pierce, Rockford IL) and the images were acquired using a Bio-Rad image analyzer (Bio-Rad, Hercules, CA).

shRNA technology to produce VEGFR2 and MMP14 knockdown cells

VEGFR2 and MMP14 knockdown in HB1.F3.CD cells were established using MISSION® VEGFR2 shRNA and MMP14 shRNA lentiviral constructs, respectively (Sigma-Aldrich, St. Louis, MO, USA). VEGFR2 knockdown efficiency was confirmed by Western Blot analysis and relative VEGFR2 mRNA expression in qRT-PCR.

Evaluation of VEGFR2 and MMP14 knockdown on NSCs' migration

To assess the effect of VEGFR2 and MMP14 on the migratory capacity of HB1.F3.CD NSCs, a wound healing assay was carried out using cell culture inserts (Ibidi, Munchen, Germany). Glioma cells were plated on one side of the chamber and NSCs with or without the respective knockdowns on the other. After cells had attached firmly, the culture insert was removed, and 1% FBS containing culture media was added to cover the cell patches (Mediatech). Migration analysis was determined by measuring the average distance traveled by the cells in different experimental conditions as compared to that of mock cells.

Quantitative RT-PCR

The relative mRNA expressions of migratory versus non-migratory NSCs as well as NSCs with shRNA-mediated knockdown of VEGFR2 were evaluated for chemoattractant receptor VEGFR2. NSCs without knockdown of MMP14 were also analyzed for expression of MMP14 transcript levels. Total cellular RNA was isolated using the RNeasy kit (Qiagen, Valencia, CA, USA) following the manufacturer's protocol, and 0.5 μg of isolated mRNA was converted to cDNA by reverse transcription using the iScript cDNA conversion kit (Bio-Rad, Hercules, CA). Quantitative PCR was conducted using the SYBR Green qPCR kit (Invitrogen, Waltham, MA, USA) and each NSC transcript was amplified in triplicates; the products were analyzed using the Bio-Rad Opticon 2 software package. Relative expression

was evaluated using the ΔC_T method (ΔC_T = C_T gene of interest- C_T GAPDH); a ΔC_T value of 3.33 was considered equivalent to a one-log change in gene expression. Expression data for migration and pretreatment experiments is presented as fold changes of the linearized ΔC_T ($2^{-\Delta CT}$) over control expression levels.

Immunohistochemistry of tissue samples

Whole brains of mice bearing tumors were dissected from the sacrificed mice and frozen in Tissue-Tek OCT (Andwin Scientific, Woodland Hills, CA) compound in a dry ice-methylbutane bath. Frozen tissues were cut coronally at the tumor injection site in two pieces and sectioned into 10 μm thick slices placed on glass histology slides. Brain sections were dried at room temperature and then followed by a fixation/permeabilization protocol carried out with 50/50 acetone-methanol. Sections were washed with cold PBS three times and blocked with 10% BSA for 30 minutes. Immunofluorescence (IF) stains were applied using primary monoclonal antibodies against VEGFR2 (1:1000, BioLegend, clone HKDR-1, San Diego, CA, USA) and h-Nestin (1:500, Covance, Princeton, NJ, USA), incubated overnight at 4ºC, washed with cold PBS 3 times, and then incubated with a secondary anti-mouse antibody for 1 hour at room temperature. The slides were washed with cold PBS 3 times, and the tissues were covered with Prolong Gold anti-fade reagent with DAPI (Life Technologies-Invitrogen, Eugene, OR, USA). Images were acquired using an inverted Axiovert200 Zeiss microscope; original objective: 20X (Carl Zeiss Microscopy, Thornwood, NY).

Flow cytometry analysis

Flow cytometry analysis was performed on migratory and non-migratory NSCs subjected to the chamber assay. After cells were collected, they were washed with PBS one time and then stained against VEGFR2 diluted in FACS buffer (1:50, 1% BSA and 0.01% sodium azide in PBS) for 45 minutes at room temperature. After washing the cells with FACS buffer three times, they were incubated for 1 hour with a secondary anti-mouse antibody at room temperature in the dark. The cells were washed again three times with FACS buffer and then analyzed using the BD LSRII-Blue machine and FACSDiva software (BD Biosciences, San Jose, CA). Analysis of the cells was presented as mean fluorescent intensity (MFI) for VEGFR2 expression.

MMP14 knockdown cells were also analyzed according to the same protocol and stained with anti-human MMP14 antibody to observe the knockdown efficiency at a protein level. The data was presented as MFI as well as the percentage of the total cell population expressing MMP14.

PCR array analysis of gene expression

Migratory and non-migratory HB1.F3.CD cells from the migration chamber assay were harvested, and total mRNA of each group was isolated using Qiagen RNeasy kit. The mRNA was converted to cDNA following the protocol provided in the User Manual for the Human Cell Motility RT^2 Profiler™ PCR Array kit (SABiosciences, Qiagen), and the samples were then applied to the actual array using the Bio-Rad Opticon 2 PCR machine. This quantitative-PCR array profiled the changes in expression of a set of 84 significant

genes associated with the cell motility comparing migratory and non-migratory NSCs. The data was analyzed accordingly with the free on-line PCR Array Data Analysis Software provided by SABiosciences.

Animal experiments

To explore the hypoxic niche within the tumor, animals were subject to intracranial stereotactic surgery. The mice were briefly anesthetized with ketamine/xylazine (115 mg/kg, 10 mg/kg), and stereotactic injections were performed using a 10 μl Hamilton syringe (Hamilton, Reno, NV, USA) and a 30-gauge needle. Two hundred and fifty thousand GBM43 cells were implanted in a 2.5 μl volume of PBS in the right hemisphere of the brain, 2.5 mm lateral to the bregma and 3 mm deep. One million HB1.F3.CD NSCs were implanted in the same manner but in the left hemisphere five days post-tumor implantation. Within 24–72 hours post NSCs' implantation, animals were sacrificed; brains were harvested and underwent serial coronal sectioning and were applied to immunohistochemistry. Representative tissue pictures were captured using an inverted Axiovert200 Zeiss microscope; original objective: 20X. (Carl Zeiss Microscopy). All animals described were cared for according to study-specific animal protocols approved by the University of Chicago Institutional Animal Care and Use Committee.

Statistical analysis

Experimental data were analyzed using GraphPad Prism Software v4.0 (GraphPad Software, San Diego, CA). Data represent the results performed in triplicate, and all experiments were executed in a blinded manner. One-way ANOVA and unpaired *t*-test were applied where applicable. Statistical significance was defined as $*p<0.05$, $**p<0.01$, and $***p<0.001$.

Results

VEGFA and MMP14 as key regulatory genes in the migratory population of HB1.F3.CD cells

To effectively identify migratory and non-migratory NSC populations, we used a transwell migration assay in which glioma-conditioned media was used as a chemo-attractant for NSCs (Fig 1A). The cells that migrated through the filter membrane and those that did not were isolated and subjected to a gene expression analysis. Two main genes were found to be upregulated in the migratory population relative to the non-migratory cells in the presence of glioma-conditioned media: VEGFA (4.9-fold) and MMP14 (5.33-fold) (Fig 1B). Relative mRNA analysis by RT-qPCR (Fig 1C) and flow cytometry analysis (Fig 1D) showed a significantly increased VEGFR2 expression in the migratory population (respectively, relative mRNA: migratory 0.76 ± 0.03 as compared to non-migratory NSCs 0.27 ± 0.01, $p<0.001$***; MFI: 970 ± 3.2 to 600 ± 4.6, $p<0.01$**). IF staining of both populations also revealed significantly higher VEGFR2 expression in the migratory population (Fig 1E). Interestingly, most of the VEGFR2 expression was localized to focal adhesion complexes of migratory HB1.F3.CD NSCs (50 ± 3.1 to 9 ± 1.4, $p<0.001$***) (Figs 1F and 1G). Focal adhesion complexes were defined as micrometer-scale subcellular structures that mediate the interactions of cells with the underlying extracellular matrix (ECM) and anchor the actin cytoskeleton to their cytoplasmic aspects [30–35]. They were identified based on previously

published protocols that use actin and phalloidin IF staining to identify anchoring points to the cellular cytoskeleton (Figs 2C and 5B) [31,33–35].

The downstream signaling of VEGF-A in migratory NSCs

Previous studies have shown that upon binding VEGF-A with its receptor VEGFR2, receptor autophosphorylation is triggered and a complex signal transduction network is activated that culminates in migration, proliferation, and inhibition of apoptosis in a variety of cells, including endothelial cells, corneal fibroblasts, oligodendrocyte precursor cells as well as cancer cells [36–39]. To assess the kinetics of VEGFR2 tyrosine phosphorylation (Tyr1175) and the activation of its downstream signals upon VEGF-A stimulation in NSCs, we measured the response to different VEGFA concentrations and durations of exposure. Our results demonstrated a dose-dependent activation of VEGF-A's downstream pathway. We observed the highest response upon treatment of HB1.F3.CD NSCs with 100 ng/ml of VEGF-A, which culminated in the up-regulation of p-VEGFR2 (Tyr1175), p-Akt, and pERK (Fig. 2A). These results suggest that dose-dependent VEGFR2 activation is transmitted downstream through MAP kinase and Akt pathways in our studied NSCs. Lysates of cells treated with 100 ng/ml of VEGF-A, collected at different time-points, showed that the activation kinetics of p-FAK (Tyr397), p-p38, and p-PCLγ1 reached its peak at 15 min (Fig. 2B, Supplementary Fig. 1). Downstream of PCLγ1, p-ERK 1/2 also achieved its peak response at 15 min. The p-Akt and the p-Src (Tyr416), however, presented a delayed response, with their highest activation at 30 min after VEGFA treatment. These data demonstrate that gradient-generated changes in VEGF-A concentration are rapidly transmitted downstream upon VEGFR2 auto-phosphorylation at Tyr1175. Interestingly, upon VEGF-A treatment, we observed the formation of actin structures concentrated in the filopodia of HB1.F3.CD NSCs, a finding that is consistent with migratory phenotype [31,33–35] (Fig. 2C, Supplementary Fig. 1). Within 15 minutes post-stimulation with VEGF-A, about 50% of NSCs demonstrated actin reorganization and a motile phenotype, represented by significantly increased migration of HB1.F3.CD NSCs in the transwell assay (21.3% ± 0.5 to 49.6% ± 3.1, $p<0.001$***) (Fig. 2D). Taken together, we conclude that VEGF-A can activate cellular signaling pathways such as FAK signaling cascade as well as promote actin filament rearrangement, known to be associated with cell motility.

VEGFR2 knockdown in HB1.F3.CD NSCs results in loss of migratory potential

Next, we examined the role of VEGF-A in regulating the tumor-tropic migratory properties of NSCs by performing a wound-healing assay with cells cultured with or without VEGF-A. We observed that VEGF-A treatment significantly increased the migration of NSCs in a dose-dependent manner (50 ± 1.2 in 0 ng/ml to 160 ± 5.3 in 100 ng/ml, $p<0.01$) (Fig. 3A). To characterize the effects of VEGFR2 knockdown in NSCs, we performed cell migration assays in shRNA-VEGFR2 and shRNA-control fluorescence-tagged NSCs. The shRNA-mediated knockdown of VEGFR2 significantly decreased VEGFR2 relative mRNA expression in NSCs (97% ± 2.1 in sh-control vs. 32% ± 2.7 in sh-VEGFR2, $p<0.01$) (Fig. 3B). The sh-VEGFR2 NSCs also showed a significant reduction in the distance traveled towards glioma cells as compared to the control shRNA (78 ± 1.2% in sh-control vs. 38 ± 2.9% in sh-VEGFR2, $p<0.01$) (Fig. 3C and D).

HB1.F3.CD cells actively track the tumor burden in vivo and maintain VEGFR2 expression

In order to examine VEGFR2 expression in migratory tumor-tracking NSCs *in vivo*, we utilized an orthotopic glioma xenograft model (Fig. 4A). Five hundred thousand HB1.F3.CD-GFP+ cells were implanted in the contralateral hemisphere of the brains of nude mice containing U87MG glioma xenografts established ten days earlier (2.5×10^5 cells/mouse). At 24 and 72 hours after NSC implantation, mice were sacrificed, and their brains were subjected to immunohistochemical analysis. We observed that within 24 hours of implantation, GFP-tagged NSCs were able to cross the midline and migrate towards the engrafted tumor in the contralateral hemisphere (Fig. 4B). At 72 hours, GFP+ NSCs were detected inside the primary tumor mass. IF staining of brain sections containing the migration route of implanted NSCs revealed that migratory carriers evenly expressed high levels of both VEGFR2 and Nestin at all three regions examined: injection site, migration route, and peritumoral region (Fig. 4C, representative IF from 5 animals). In addition, migratory NSCs were able to maintain high expression levels of the stem cell-associated marker Nestin throughout their path towards the tumor [11].

MMP14 as a downstream target of VEGF-A in HB1.F3.CD NSCs

Interaction between MMP14 and VEGFR2 has been previously demonstrated in cancer cells [40]. Our preliminary analysis of the migratory subpopulation of NSCs revealed that both VEGF-A and MMP14 were significantly upregulated. Based on this, we next set to investigate the existence of a possible link between VEGF-A and MMP14. We first set up a time-course treatment of NSCs using the dose of VEGF-A established above (100 ng/ml). Lysates were collected at 0, 15, 30, 60, and 90 min after treatment, and protein expression was measured by western blot analysis. We found that both VEGFR2 (Tyr1175) and MMP14 had their peak activation 30–45 min after initial therapy (Fig. 5A). We also observed a similar induction of MMP14 post-VEGF-A stimulation by IF analysis (Fig. 5B). Next, to confirm that the high MMP14 expression was directly related to VEGF-A treatment and VEGFR2 activation, we knocked down VEGFR2 expression in our studied HB1.F3.CD NSCs. Pure shRNA-VEGFR2 populations and shRNA-controls were treated with 100 ng/ml of VEGF-A for 15 min (Fig. 5C). As expected, our data revealed attenuated VEGFR2 expression and significantly diminished p-Akt expression in VEGFR2 knockdown cells. This finding confirms that a successful gene knockdown was accomplished, as p-Akt is a direct downstream target of VEGFR2 and was also significantly attenuated post-VEGFA stimulation. Moreover, we found decreased levels of MMP14 expression in sh-VEGFR2 cells, which suggests that MMP14 activation is controlled by and is a downstream target of VEGFR2.

MMP14 is also required for NSC migration

To assess the importance of MMP14 within the context of NSC migration, we knocked down the MMP14 gene in HB1.F3.CD cells (Fig 6A). Next, we performed a wound-healing assay using HB1.F3.CD shRNA-control, shRNA-MMP14 #2, shRNA-MMP14 #3, and shRNA-MMP14 #4 NSCs towards U87 glioma cells (Fig. 6B and C). The knockdown and the shRNA control cells were placed in the chamber well 200 μM away from a well that contains U87 glioma line and wound healing assay were performed. The distance traveled

by the NSCs with different manipulations were photograph every two hours for 24 hours and the representative images shown in figure 6B. The percent travel was measured at 24 hours as shown in figure 6C. We observed a significant decrease in NSC migration in all shRNA-MMP14 groups (43 ± 3.4 in shRNA-control, 11 ± 1.3 in shRNA-MMP14 #2, 38 ± 3.9 in shRNA-MMP14 #3 and 19 ± 2.2 in shRNA-MMP14 #4), with shRNA-MMP14 #2 expressing the lowest migration rate. These data suggest that downstream activation of MMP14 is a required step for optimal NSC migration towards neoplastic areas.

Discussion

The role of NSCs as therapeutic carriers against malignant brain tumors has been widely studied and well established [9,11–13,17]. Due to their safety profile, inherent tumor-tropism, and immunosuppressive properties, HB1.F3.CD NSCs are considered one of the optimal carriers for anti-cancer therapeutics and have recently entered a Phase I clinical trial for patients with recurrent malignant gliomas (NCT01172964). However, the major obstacle for the clinical application of NSC-based anti-cancer therapies is the small fraction of carrier cells that possess tumor-tropic migratory capacities in preclinical animal models [4,19–22]. Here, our main goal is to understand why some NSCs can effectively migrate and deliver their therapeutic payload to targeted tumor areas while others are not. To better comprehend this process, we examined both migratory and non-migratory NSC populations in vitro and in vivo. We closely assessed their mechanism and route of migration, and through gene expression analysis we identified two essential genes were driving this process: VEGF-A and MMP14.

Recent research suggests that NSCs' tropism towards neoplastic areas is driven by chemoattractants produced at the tumor site. The intratumoral hypoxic microenvironment activates SDF-1/CXCR4 and VEGF/VEGFR signaling pathways together with MMPs, which may act as downstream effectors to increase NSC tropism [18,20,41–43]. We found that VEGFR2 expression was critical for the tumor-tropic migratory properties of HB1.F3.CD NSCs. Further analysis showed that the highest VEGFR2 expression was concentrated at focal adhesion complexes and filopodia of migratory cells. This suggests that VEGF-A-mediated cytoskeletal reorganization is present in our studied migratory population. These data are in line with previously published studies that show VEGFA-mediated actin reorganization and filopodia formation in migratory endothelial and oligodendrocyte precursor cells [2,39,44].

We further assessed the activation of VEGF-A downstream pathways in our migratory NSCs and their collective role in NSC migration. First, we observed VEGF-A-mediated phosphorylation and activation of VEGF-A's binding site, p-VEGFR2 (Tyr1175). Previous publications described Tyr1175 as being responsible for linking VEGF-A receptor phosphorylation to signal transduction. PLCγ, an upstream kinase that requires Src binding for its activation, was shown to bind the intracellular domain of VEGFR2, leading to activation of the MAP kinase ERK1/2 signaling pathway. PLCγ and ERK1/2 activation lead to podosome formation, cell migration, and proliferation [19,45]. Similarly, our results indicated downstream activation of Src, PLCγ1, and MAP kinase ERK1/2 upon VEGF-A stimulation. We additionally noted high levels of activated p38 in migratory NSCs upon

VEGF-A treatment. This finding is consistent with previously published materials that point to VEGF-induced activation of p38 and ERK1/2 as a possible mechanism of focal adhesion and podosome formation in migratory cells [44]. We further observed downstream activation of Akt in migratory cells, achieving its peak 30 min after VEGF-A stimulation. Similarly, other publications have demonstrated a VEGF-mediated activation of Akt, a kinase pathway linked to increased migration and inhibition of apoptosis in endothelial cells [37,46]. Lastly, we also detected strong FAK activation in migratory NSCs. In agreement with our results, Src was previously shown to bind FAK, leading to increased migration of both oligodendrocyte precursors and endothelial cells. In addition, FAK has been shown to regulate focal adhesion turnover during cell migration and to regulate cell survival [47]. Previously published mechanisms of VEGF-mediated downstream pathway activation have been described in endothelial cells, corneal fibroblasts, oligodendrocyte precursor cells, and cancer cells [36–39]. Our results suggest that VEGF-A-dependent downstream activation of PLCγ1, Akt, and FAK in NSCs may be directly related to cytoskeletal reorganization, podosome formation, and cell migration. This explains our observation of increased VEGFR2 expression in focal adhesion areas of migratory NSCs. This mechanism highlights the upstream signaling pathways that are likely driving the observed differential migratory capacities in NSCs expressing higher levels of VEGFR2.

We next studied the role of MMP14 in NSCs' targeted migration towards diffuse tumor foci. We found that MMP14 was required for NSC migration and that its expression is dependent on VEGFR2 activation in migratory NSCs. Knockdown of VEGFR2 completely blocked MMP14 expression and significantly impaired migration of HB1.F3.CD NSCs. We have thus demonstrated, for the first time, that MMP14 is a possible downstream target of activated VEGFR2 in migratory NSCs. This finding is in agreement with previously published data that showed that decreased MMP14 activity inhibited the migration of human bone marrow MSCs [48]. The same study also revealed that MMP14 overexpression had the capacity to restore MSC migration. Additional reports observed VEGF-induced MMP activation and extracellular matrix degradation in endothelial cells [2]. Interestingly, several other studies indicated that a reverse pathway was present in malignant cells, including malignant glioma and breast cancer models, where MMP14 was noted to regulate VEGF-A expression through a complex with VEGFR2 and Src, leading to increased xenograft growth and tumor-related angiogenesis [37]. Thus, it is conceivable that in the NSC line the autocrine upregulation of MMP14, mediated by VEGFA/VEGFR2 signaling, is responsible for targeted NSC migration towards malignant areas. Much interest has been placed on various niches that may populate the landscape of malignant gliomas and represent distinct tumor microenvironments, among them hypoxic regions that have been shown to secrete higher levels of VEGF-A and, in turn, attract migratory NSCs. Therefore, it is possible that constant VEGF-A expression may also activate intrinsic VEGFR2 activity in migratory cells in an autocrine manner. This leads to downstream MMP14 expression, remodeling of extracellular matrix, and increased directional migration of carrier cells to areas of pathology. This is an important finding since a consistent activation of MMP14 would enhance the directional migration of NSC carriers towards infiltrative tumor foci and would also increase the overall number of carriers that effectively reach and distribute within the

malignant area. Such funding provides us the rational of modifying the NSC-based cell carrier to overexpress the molecule like MMP14 to enhance their tumor homing capacity.

Numerous groups have shown that in order to serve as viable cell carriers, NSCs must retain their selective tumor-tropic properties, long-term survival capability, and the ability to successfully reach the targeted tissue into which they distribute their payload [4,11,49]. Data presented in this report indicate that within 72 hours of implantation HB1.F3.CD NSC carriers were able to migrate to the contralateral cerebral hemisphere and effectively home to the tumor bed. Analysis of both migratory and non-migratory NSC populations revealed that migratory NSCs consistently expressed high levels of VEGFR2 and Nestin throughout the entirety of their migratory path. These findings are in keeping with previous reports that show that migratory NSCs survive and possibly maintain their stemness during the migration, further supporting their utility as robust cell carriers [4,9,11,18].

Conclusion

Our results indicate that functional MMP14 expression is required for tumor-tropic migration of NSC carriers. We also present MMP14 as a possible downstream target for VEGFR2 in migratory NSCs. This suggests that VEGFR2 downstream signaling activation could be a contributory mechanism underlying the increased motility of migratory NSCs. Thus, MMP14 modulation may constitute a novel target to enhance migration and delivery capacity of NSCs to targeted disease areas, allowing for future improvements in the therapeutic efficacy of these delivery vehicles and augmentation of their translational potential.

Supplementary Material

Refer to Web version on PubMed Central for supplementary material.

Acknowledgments

We thank Lingjiao Zhang for her assistance on statistical analysis. This work was supported by R00 CA160775, The authors declare no conflict of interest.

References

1. Brandes AA, Fiorentino MV. The role of chemotherapy in recurrent malignant gliomas: an overview. Cancer Invest. 1996; 14:551–9. [PubMed: 8951359]
2. Laquintana V, Trapani A, Denora N, Wang F, Gallo JM, Trapani G. New strategies to deliver anticancer drugs to brain tumors. Expert Opin Drug Deliv. 2009; 6:1017–32. [PubMed: 19732031]
3. Ahmed AU, Alexiades NG, Lesniak MS. The use of neural stem cells in cancer gene therapy: predicting the path to the clinic. Curr Opin Mol Ther. 2010; 12:546–52. [PubMed: 20886386]
4. Ahmed AU, Tyler MA, Thaci B, et al. A comparative study of neural and mesenchymal stem cell-based carriers for oncolytic adenovirus in a model of malignant glioma. Mol Pharm. 2011; 8:1559–72. [PubMed: 21718006]
5. Ahmed AU, Lesniak MS. Glioblastoma multiforme: can neural stem cells deliver the therapeutic payload and fulfill the clinical promise? Expert Rev Neurother. 2011; 11:775–7. [PubMed: 21651324]
6. Young JS, Kim JW, Ahmed AU, Lesniak MS. Therapeutic cell carriers: a potential road to cure glioma. Expert Rev Neurother. 2014; 14:651–60. [PubMed: 24852229]

7. Gage FH, Temple S. Neural stem cells: generating and regenerating the brain. Neuron. 2013; 80:588–601. [PubMed: 24183012]
8. Aboody KS, Najbauer J, Metz MZ, et al. Neural stem cell-mediated enzyme/prodrug therapy for glioma: preclinical studies. Sci Transl Med. 2013; 5:184ra59.
9. Aboody KS, Brown A, Rainov NG, et al. Neural stem cells display extensive tropism for pathology in adult brain: evidence from intracranial gliomas. Proc Natl Acad Sci U S A. 2000; 97:12846–51. [PubMed: 11070094]
10. Benedetti S, Pirola B, Pollo B, et al. Gene therapy of experimental brain tumors using neural progenitor cells. Nat Med. 2000; 6:447–50. [PubMed: 10742153]
11. Ahmed AU, Thaci B, Tobias AL, et al. A preclinical evaluation of neural stem cell-based cell carrier for targeted antiglioma oncolytic virotherapy. J Natl Cancer Inst. 2013; 105:968–77. [PubMed: 23821758]
12. Auffinger B, Morshed R, Tobias A, Cheng Y, Ahmed AU, Lesniak MS. Drug-loaded nanoparticle systems and adult stem cells: a potential marriage for the treatment of malignant glioma? Oncotarget. 2013; 4:378–96. [PubMed: 23594406]
13. Thaci B, Ahmed AU, Ulasov IV, et al. Pharmacokinetic study of neural stem cell-based cell carrier for oncolytic virotherapy: targeted delivery of the therapeutic payload in an orthotopic brain tumor model. Cancer Gene Ther. 2012; 19:431–42. [PubMed: 22555507]
14. Yip S, Aboody KS, Burns M, et al. Neural stem cell biology may be well suited for improving brain tumor therapies. Cancer J. 2003; 9:189–204. [PubMed: 12952304]
15. Shah K, Bureau E, Kim DE, et al. Glioma therapy and real-time imaging of neural precursor cell migration and tumor regression. Ann Neurol. 2005; 57:34–41. [PubMed: 15622535]
16. Mader EK, Maeyama Y, Lin Y, et al. Mesenchymal stem cell carriers protect oncolytic measles viruses from antibody neutralization in an orthotopic ovarian cancer therapy model. Clin Cancer Res. 2009; 15:7246–55. [PubMed: 19934299]
17. Ahmed AU, Thaci B, Alexiades NG, et al. Neural stem cell-based cell carriers enhance therapeutic efficacy of an oncolytic adenovirus in an orthotopic mouse model of human glioblastoma. Mol Ther. 2011; 19:1714–26. [PubMed: 21629227]
18. Aboody KS, Najbauer J, Schmidt NO, et al. Targeting of melanoma brain metastases using engineered neural stem/progenitor cells. Neuro Oncol. 2006; 8:119–26. [PubMed: 16524944]
19. Lee DH, Ahn Y, Kim SU, et al. Targeting rat brainstem glioma using human neural stem cells and human mesenchymal stem cells. Clin Cancer Res. 2009; 15:4925–34. [PubMed: 19638465]
20. Zhao D, Najbauer J, Garcia E, et al. Neural stem cell tropism to glioma: critical role of tumor hypoxia. Mol Cancer Res. 2008; 6:1819–29. [PubMed: 19074827]
21. Jeon JY, An JH, Kim SU, Park HG, Lee MA. Migration of human neural stem cells toward an intracranial glioma. Exp Mol Med. 2008; 40:84–91. [PubMed: 18305401]
22. Kim JH, Lee JE, Kim SU, Cho KG. Stereological analysis on migration of human neural stem cells in the brain of rats bearing glioma. Neurosurgery. 2010; 66:333–42. discussion 42. [PubMed: 20087133]
23. Imitola J, Raddassi K, Park KI, et al. Directed migration of neural stem cells to sites of CNS injury by the stromal cell-derived factor 1alpha/CXC chemokine receptor 4 pathway. Proc Natl Acad Sci U S A. 2004; 101:18117–22. [PubMed: 15608062]
24. Schmidt NO, Przylecki W, Yang W, et al. Brain tumor tropism of transplanted human neural stem cells is induced by vascular endothelial growth factor. Neoplasia. 2005; 7:623–9. [PubMed: 16036113]
25. Xu Q, Wang S, Jiang X, et al. Hypoxia-induced astrocytes promote the migration of neural progenitor cells via vascular endothelial factor, stem cell factor, stromal-derived factor-1alpha and monocyte chemoattractant protein-1 upregulation in vitro. Clin Exp Pharmacol Physiol. 2007; 34:624–31. [PubMed: 17581219]
26. Lamszus K, Lengler U, Schmidt NO, Stavrou D, Ergun S, Westphal M. Vascular endothelial growth factor, hepatocyte growth factor/scatter factor, basic fibroblast growth factor, and placenta growth factor in human meningiomas and their relation to angiogenesis and malignancy. Neurosurgery. 2000; 46:938–47. discussion 47–8. [PubMed: 10764269]

27. Kim SK, Kim SU, Park IH, et al. Human neural stem cells target experimental intracranial medulloblastoma and deliver a therapeutic gene leading to tumor regression. Clin Cancer Res. 2006; 12:5550–6. [PubMed: 17000692]
28. Kitange GJ, Carlson BL, Mladek AC, et al. Evaluation of MGMT promoter methylation status and correlation with temozolomide response in orthotopic glioblastoma xenograft model. J Neurooncol. 2009; 92:23–31. [PubMed: 19011762]
29. Sonabend AM, Ulasov IV, Tyler MA, Rivera AA, Mathis JM, Lesniak MS. Mesenchymal stem cells effectively deliver an oncolytic adenovirus to intracranial glioma. Stem Cells. 2008; 26:831–41. [PubMed: 18192232]
30. Izzard CS, Lochner LR. Formation of cell-to-substrate contacts during fibroblast motility: an interference-reflexion study. Journal of cell science. 1980; 42:81–116. [PubMed: 7400245]
31. Gardel ML, Schneider IC, Aratyn-Schaus Y, Waterman CM. Mechanical integration of actin and adhesion dynamics in cell migration. Annu Rev Cell Dev Biol. 2010; 26:315–33. [PubMed: 19575647]
32. Wolfenson H, Lavelin I, Geiger B. Dynamic regulation of the structure and functions of integrin adhesions. Dev Cell. 2013; 24:447–58. [PubMed: 23484852]
33. Geiger B, Spatz JP, Bershadsky AD. Environmental sensing through focal adhesions. Nat Rev Mol Cell Biol. 2009; 10:21–33. [PubMed: 19197329]
34. Albiges-Rizo C, Destaing O, Fourcade B, Planus E, Block MR. Actin machinery and mechanosensitivity in invadopodia, podosomes and focal adhesions. Journal of cell science. 2009; 122:3037–49. [PubMed: 19692590]
35. Chorev DS, Moscovitz O, Geiger B, Sharon M. Regulation of focal adhesion formation by a vinculin-Arp2/3 hybrid complex. Nat Commun. 2014; 5:3758. [PubMed: 24781749]
36. Olsson AK, Dimberg A, Kreuger J, Claesson-Welsh L. VEGF receptor signalling - in control of vascular function. Nat Rev Mol Cell Biol. 2006; 7:359–71. [PubMed: 16633338]
37. Deryugina EI, Soroceanu L, Strongin AY. Up-regulation of vascular endothelial growth factor by membrane-type 1 matrix metalloproteinase stimulates human glioma xenograft growth and angiogenesis. Cancer Res. 2002; 62:580–8. [PubMed: 11809713]
38. Han KY, Fahd DC, Tshionyi M, et al. MT1-MMP modulates bFGF-induced VEGF-A expression in corneal fibroblasts. Protein Pept Lett. 2012; 19:1334–9. [PubMed: 22670674]
39. Hayakawa K, Pham LD, Som AT, et al. Vascular endothelial growth factor regulates the migration of oligodendrocyte precursor cells. J Neurosci. 2011; 31:10666–70. [PubMed: 21775609]
40. Eisenach PA, Roghi C, Fogarasi M, Murphy G, English WR. MT1-MMP regulates VEGF-A expression through a complex with VEGFR-2 and Src. Journal of cell science. 2010; 123:4182–93. [PubMed: 21062896]
41. Ingraham CA, Park GC, Makarenkova HP, Crossin KL. Matrix metalloproteinase (MMP)-9 induced by Wnt signaling increases the proliferation and migration of embryonic neural stem cells at low O2 levels. J Biol Chem. 2011; 286:17649–57. [PubMed: 21460212]
42. Rosova I, Dao M, Capoccia B, Link D, Nolta JA. Hypoxic preconditioning results in increased motility and improved therapeutic potential of human mesenchymal stem cells. Stem Cells. 2008; 26:2173–82. [PubMed: 18511601]
43. Liu H, Xue W, Ge G, et al. Hypoxic preconditioning advances CXCR4 and CXCR7 expression by activating HIF-1alpha in MSCs. Biochem Biophys Res Commun. 2010; 401:509–15. [PubMed: 20869949]
44. Rousseau S, Houle F, Landry J, Huot J. p38 MAP kinase activation by vascular endothelial growth factor mediates actin reorganization and cell migration in human endothelial cells. Oncogene. 1997; 15:2169–77. [PubMed: 9393975]
45. Takeuchi H, Natsume A, Wakabayashi T, et al. Intravenously transplanted human neural stem cells migrate to the injured spinal cord in adult mice in an SDF-1- and HGF-dependent manner. Neurosci Lett. 2007; 426:69–74. [PubMed: 17884290]
46. Morales-Ruiz M, Fulton D, Sowa G, et al. Vascular endothelial growth factor-stimulated actin reorganization and migration of endothelial cells is regulated via the serine/threonine kinase Akt. Circ Res. 2000; 86:892–6. [PubMed: 10785512]

47. Ilic D, Kovacic B, Johkura K, et al. FAK promotes organization of fibronectin matrix and fibrillar adhesions. Journal of cell science. 2004; 117:177–87. [PubMed: 14657279]

48. Malinowski M, Pietraszek K, Perreau C, et al. Effect of lumican on the migration of human mesenchymal stem cells and endothelial progenitor cells: involvement of matrix metalloproteinase-14. PLoS One. 2012; 7:e50709. [PubMed: 23236386]

49. Carney BJ, Shah K. Migration and fate of therapeutic stem cells in different brain disease models. Neuroscience. 2011; 197:37–47. [PubMed: 21946010]

Highlight

1. We investigated the mechanisms of tumor-tropic migration of an FDA-approved NSC line, HB1.F3.CD.
2. Gene expression analysis and identified vascular endothelial growth factor-A (VEGFA) and membrane-bound matrix metalloproteinase, MMP14, as molecules those expressions are significantly elevated in the migratory NSCs.
3. Our results suggest, for the first time, involvement of VEGFR2-regulated MMP14 in the tumor-tropic migratory behavior of NSCs

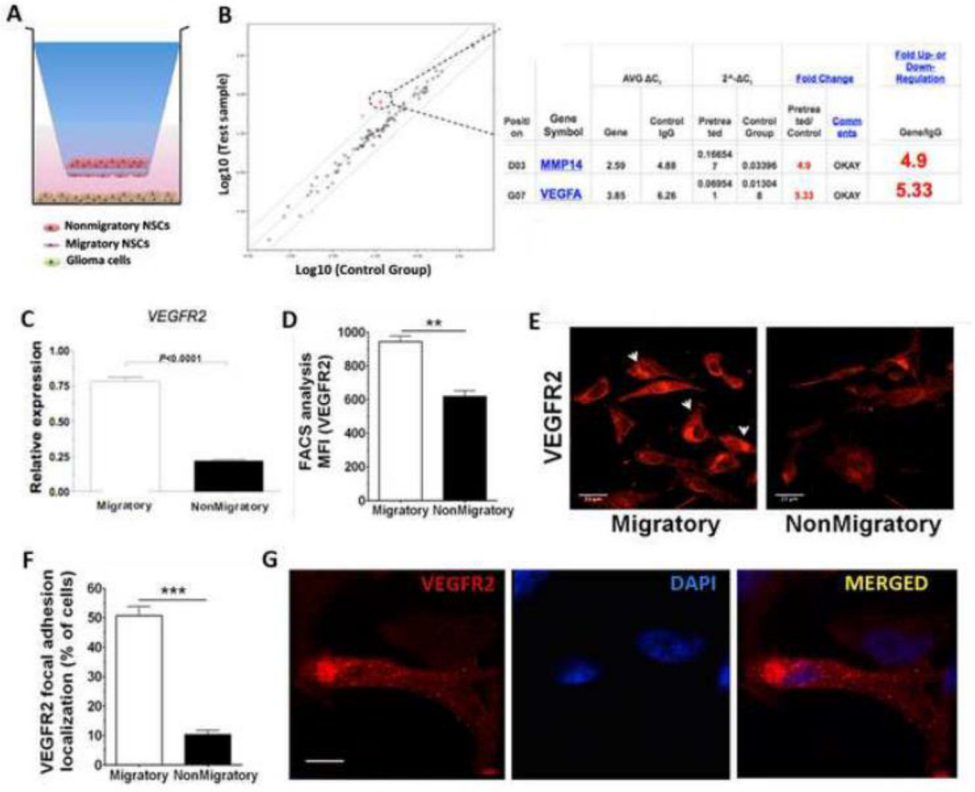

Figure 1. VEGFA and MMP14 as the main regulatory genes in migratory HB1.F3.CD NSC populations

(A) Experimental scheme. Migratory and non-migratory NSC populations were identified through the use of a transwell migration assay in which glioma-conditioned media was used as a chemoattractant for NSCs. **(B)** Both migratory and non-migratory NSC populations were isolated and subjected to a PCR array containing 84 genes related to cell migration. Graph showing the correlation between fold changes in gene expression in both populations. Black and gray dots represent upregulated or downregulated genes with a fold change >3, respectively. **(C)** RT-PCR analysis of relative mRNA expression of VEGFR2. Gene expression levels were normalized to GAPDH, a ubiquitous control RNA. **(D)** VEGFR2 protein expression in both migratory and non-migratory NSC populations. Cells were incubated on ice with APC-conjugated anti-VEGFR2 antibody or control IgG1 and analyzed by flow cytometry. MFI, geometric mean of fluorescence intensity. **(E)** IF staining of both isolated populations for VEGFR2 marker. DNA was stained with DAPI. Scale bars, 23 μm. **(F)** Quantification of the experiment presented in (E). Approximately 300 cells were analyzed per condition (n=4). **(G)** Magnified views of focal adhesion areas in HB1.F3.CD migratory NSCs expressing VEGFR2 marker. DNA was stained with DAPI. Scale bars, 100 μm. The values shown are mean ± SEM. *, $P < 0.05$; **, $P < 0.01$; versus control.

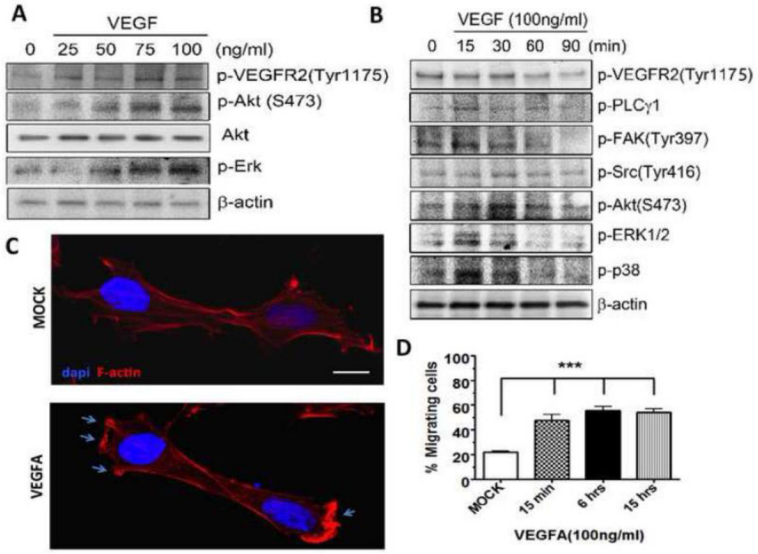

Figure 2. Concentration, temporal integration of VEGF-A signal, and its downstream regulation

(A) Western blot detection of the indicated proteins in HB1.F3.CD NSCs treated with concentration range (0 to 100 ng/ml) of VEGF and collected at 15 min post-treatment. **(B)** Western blot analysis showing time-dependent expression (0 to 90 min) of VEGFR2 downstream kinases. β-actin is shown as a loading control. **(C)** VEGFA-induced actin cytoskeleton reorganization. HB1.F3.CD cells plated on gelatin-coated chamber slides were treated with vehicle (mock) or were exposed to 100 ng/ml VEGFA for 6 hours. Cells were fixed and permeabilized, and F-actin content was detected using phalloidin conjugated with rhodamin. Coverslips were mounted onto microscope slides and analyzed under a confocal microscope (Zeiss LSM 510). The pictures shown are representative of at least 15 different fields observed in each experiment and of two similar independent experiments. **(D)** Quantification of the percentage of migrating cells per field in the experiment presented in (C). The values shown are mean ± SEM. ***, P <0.001; versus mock.

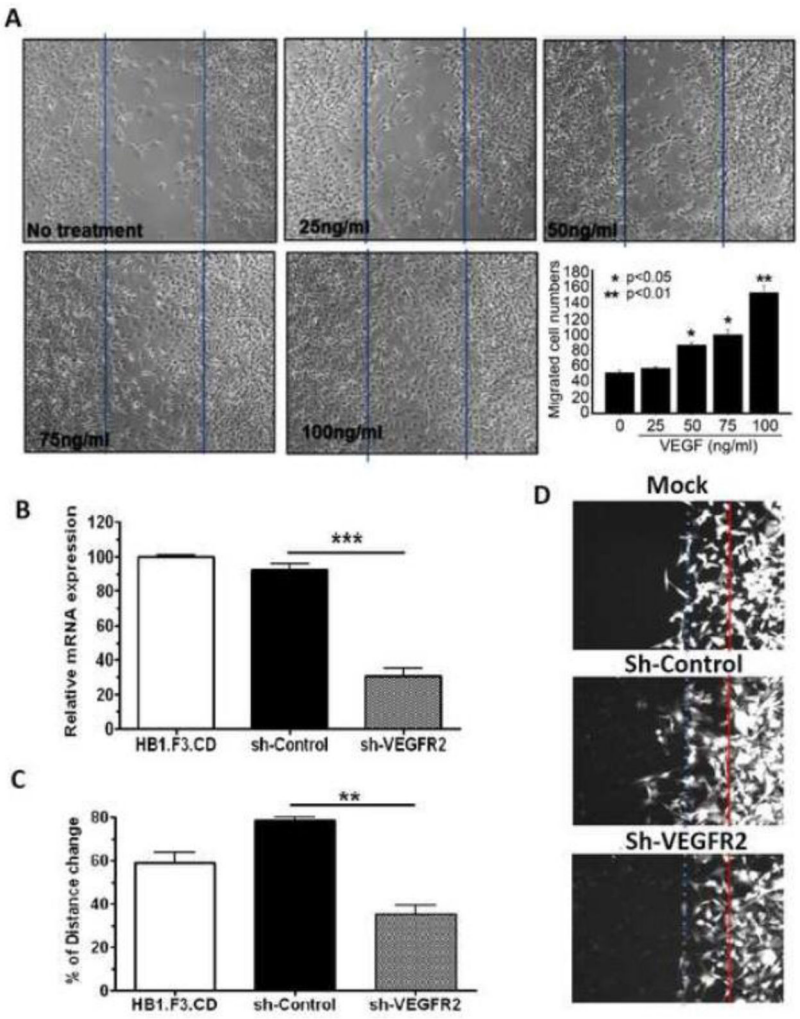

Figure 3. HB1.F3.CD cells submitted to VEGFR2 knockdown lose their migration potential

(A) Wound healing assay using HB1.F3.CD NSCs treated with a range of concentrations of VEFGA (0, 25, 50, 75, and 100 ng/ml) against U87 glioma cells. Representative photographs taken at 24h post-wound (40X). The wound closure was quantified at 24h post-wound by measuring the remaining unmigrated area using ImageJ. **(B)** RT-PCR analysis of relative mRNA expression of VEGFR2 in HB1.F3.CD, sh-control, and sh-VEGFR2 NSCs. Gene expression levels were normalized to GAPDH, a ubiquitous control RNA. **(C)** The wound closure was quantified at 24h post-wound by measuring the remaining unmigrated area using ImageJ. The values shown are mean ± SEM. *, $P < 0.05$; **, $P < 0.01$; ***, $P < 0.001$; versus control. **(D)** Wound-healing assay using HB1.F3.CD NSCs, sh-control, and sh-VEGFR2 fluorescence-tagged NSCs to assess the effect of VEGFR2 on the migratory capacity of NSCs towards glioma cells.

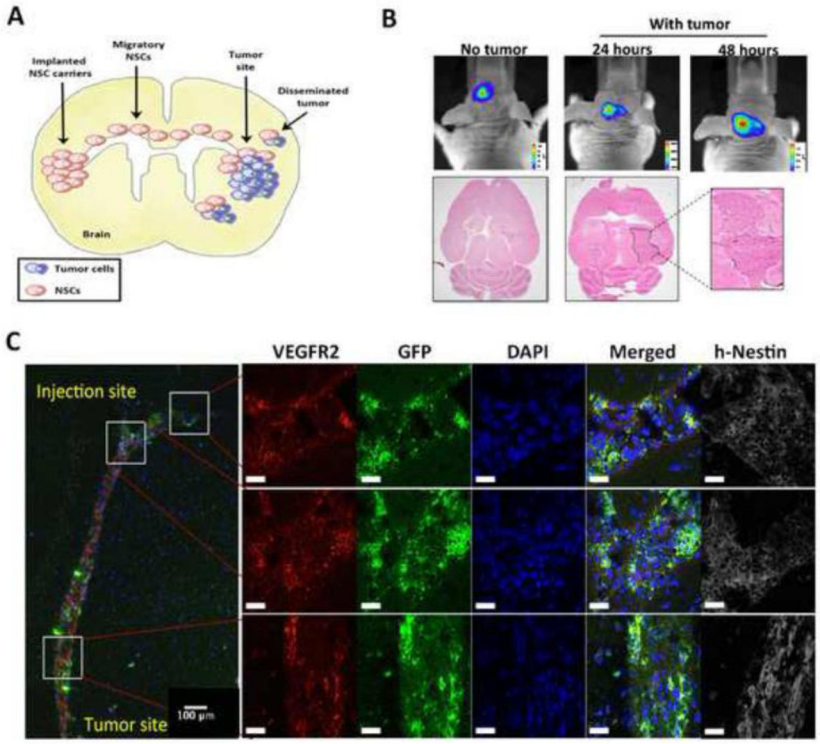

Figure 4. HB1.F3.CD NSCs actively track malignant areas in vivo and maintain their stemness and VEGFR2 expression during migration

(A) Experimental scheme. *In vivo* analysis of both migratory and non-migratory NSC populations. Briefly, 5×10^5 HB1.F3.CD-GFP+ NSCs were implanted in the contralateral hemisphere of nude mouse brains containing U87MG glioma xenografts established 10 days earlier (2.5×10^5 cells/mouse). At 24 and 72 hours after NSC implantation, mice were sacrificed and their brains were subjected to immunohistochemical analysis. **(B)** *In vivo* tumor-tropic migration of HB1.F3.CD stably expressing luciferase (Luc) gene. Bioluminescent imaging of mice after intracranial injection of HB1.F3.CD-Luc into the left hemisphere of the mice implanted with U87 xenograft tumors on the right side (Left two panels) 7 days post implantation. **(C)** IF staining of the NSCs' migration path with anti-VEGFR2 and anti-Nestin antibodies. DNA was stained with DAPI. Scale bars, 100 μm. Magnified views of migratory NSCs expressing VEGFR2 and Nestin markers. Scale bars, 100 μm.

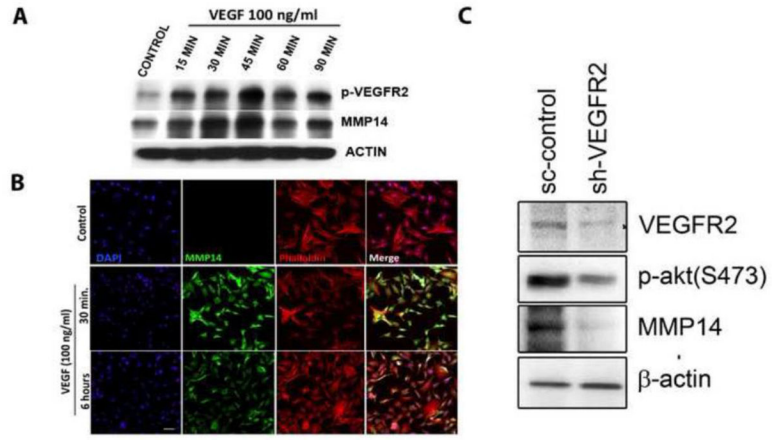

Figure 5. MMP14 as a novel downstream target of VEGFA in HB1.F3.CD NSCs

(A) Time-course treatment of NSCs using the established VEGFA dose of 100 ng/ml. Lysates were collected at 0, 15, 30, 60, and 90 min after treatment, and protein expression was measured by western blotting. **(B)** IF staining of HB1.F3.CD cells treated with 100ng/ml of VEGFA for 15 minutes and untreated controls; anti-human MMP14 (FITC), anti-human phalloidin (APC); DNA was stained with DAPI. **(C)** Western blot analysis showing the expression of VEGFR2 downstream kinases in sh-control and sh-VEGFR2 HB1.F3.CD NSCs. β-actin is shown as a loading control.

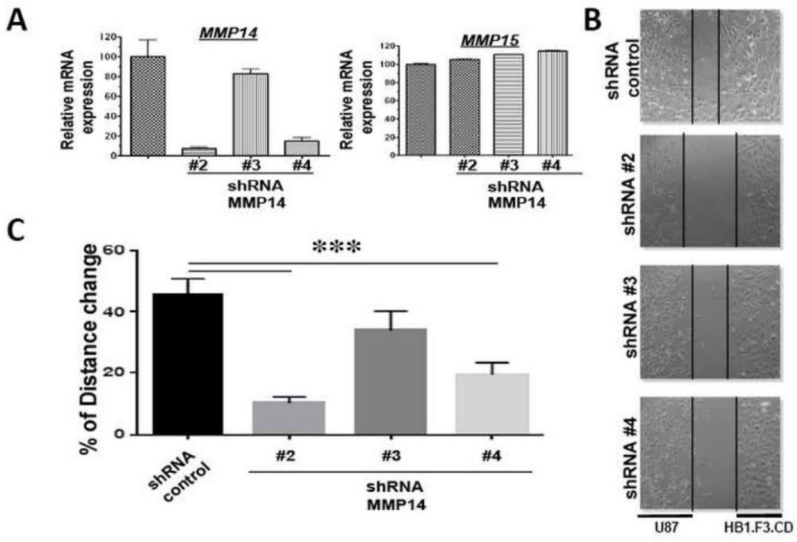

Figure 6. MMP14 is required for tumor tropic migration HB1.F3.CD NSCs

(A) RT-PCR analysis of relative mRNA expression of MMP14 (left) and MMP15 (right) in HB1.F3.CD with sh-control and three different MMP14 shRNA (#2, #3, and #4). Gene expression levels were normalized to GAPDH, a ubiquitous control RNA. **(B)** Wound healing assay using HB1.F3.CD sh-control, sh-MMP14 #2, sh-MMP14 #3, and sh-MMP14 #4 NSCs against U87 glioma cells. Representative photographs taken at 24h post-wound (40X). **(C)** The wound closure in the experiment present in (B) was quantified 24h post-wound by measuring the remaining unmigrated area using ImageJ. The values shown are mean ± SEM. *, $P < 0.05$; **, $P < 0.01$; ***, $P < 0.001$; versus control.